Performance and application of direct laser welding of Al-Si coated PHS with specialized filler wire without pretreatment

Xuzhi Zhang[1,a], Wu Tao[1], Jiazhi Zhang[1] and Shanglu Yang[1,.2,b,†]

[1]*Shanghai Institute of Optics and Fine Mechanics, Chinese Academy of Science, Shanghai 201800, China*

[2]*Center of Materials Science and Optoelectronics Engineering, University of Chinese Academy of Sciences, Beijing 100049, China*

Email: [a]zhangxuzhi@siom.ac.cn, [†]yangshanglu_lab@126.com

In the automotive industry, the Al-Si coating attached to the press-hardened steel (PHS) around the tailored edge was removed before laser tailor welding to prevent the formation of Al-rich ferrite in the weld zone (WZ), which weakened the mechanical properties. However, eliminating the Al-Si coating process entails high equipment costs and license fees. This study introduced an innovative direct laser-filler wire welding technique for Al-Si coated PHS, enabling high-quality laser welding of seven distinct Al-Si coated PHSs with varying plate thicknesses, coating thicknesses and base metal (BM) strength. Weld reinforcement was controlled within 6% to 17%. After hot stamping, the tensile strength and elongation of the welded joints were over 1500 MPa and 7%, respectively. Additionally, the average microhardness values of the WZs were comparable to that of the BM. High-speed tensile tests on the welded joints of PHS with thick or thin Al-Si coating revealed that the tensile strength exceeded 1500 MPa and failed in BM. This technology has been applied to large-scale production of automotive A-pillars, B-pillars, one-piece door rings, and other components.

Keywords: Al-Si coating; Press-hardened steel; Laser welding; Filler wire.

1. Introduction

Press-hardened steel (PHS) is one of the essential lightweight materials for the automotive industry due to its advantages of lightweight, high strength, high hardened forming accuracy, and low hardened spring back at high temperatures [1,2]. PHS's ultimate tensile strength reaches 1500MPa. Al-Si coatings are widely used in PHS due to their excellent resistance to corrosion and oxidation [3-5].

Laser beams were used in the automotive industry to weld PHS and reduce vehicle weight and cost. However, the Al element in the coating entered the weld and formed segregation, affecting the microstructure and mechanical properties of the weld. Martin [6] *et al.* studied the austenite formation process in low-manganese steels with varying Al contents (0.02 wt.%, 0.48 wt.%, and 0.94 wt.%) under continuous heating conditions, discovering that an increase in the Al content stabilized the ferrite phase. Ding [7] *et al.* found that the melting and movement of the Al-Si coating to the molten pool can trigger the formation of ferrite in the weld zone (WZ) of the laser-welded joint of Al-Si coated PHS, and the type of ferrite was clarified to be δ-ferrite. According to Saha [8] *et al.*, transmission electron microscopy revealed that δ-ferrite and martensite are the primary microstructures in the weld after laser welding, and the non-equilibrium δ-ferrite phase

© The Author(s) 2024

Y. Zhang and M. Ma (eds.), *Proceedings of the 7th International Conference on Advanced High Strength Steel and Press Hardening (ICHSU 2024)*, Atlantis Highlights in Materials Science and Technology 3,
https://doi.org/10.2991/978-94-6463-581-2_71

transformed into α-ferrite after hot stamping. Moreover, their evaluations of the nano hardness and tensile properties of welded joints after hot stamping showed that ferrite was the primary cause of the softening and degradation of tensile properties in welded joints [9]. Xu [10] *et al.* reduced ferrite formation by incorporating austenitizing elements into a wire. The elements transitioned continuously and steadily to the molten pool through a liquid-bridge transition, simultaneously diluting the aluminum elements in the molten pool. This process results in a fully martensitic weld after hot stamping.

Numerous scholars have conducted extensive research to address the issue of aluminum segregation in welds caused by Al-Si coating. At present, the primary methods to reduce or prevent the formation of aluminum segregation in the weld include removing the Al-Si coating layer before welding [11,12], optimizing the welding process parameters [13,14], enhancing the mobility of the molten pool [15,16], modifying the Al-Si coating layer [17], incorporating intermediate interlayers [18], and filler wires [19]. The above methods can inhibit or reduce ferrite formation and improve the mechanical properties of welded joints. But for the Al-Si coated PHS with different plate thicknesses, coating thicknesses, and base metal strength, there are apparent limitations: low welding efficiency, poor weld seam forming quality and forming performance, destructive mechanical properties of welded joints and poor stability, which cannot meet the needs of a variety of PHS welding under the premise of ensuring the quality of welding. Welding Al-Si coated PHS from seven original equipment manufacturers was achieved without removing the coating or setting gaps. Practical applications in automobile production are presented.

2. Experimental Procedure

Seven different types of Al-Si coated PHS were selected as the experimental materials. Each PHS's chemical compositions (wt.%), plate thicknesses (mm), and coating thicknesses (μm) before hot stamping were shown in Table 1, Table 2, and Table 3, respectively. The tensile strengths of PHS #1~#6 were 1500 MPa after hot stamping, while #7 was 1700 MPa.

The IPG YLS-10000 fiber laser system, KUKA robot, and Fronius KD7000 wire feeder were used for the experiment without shielding gas protection. The laser wavelength was 1070 nm, and the focal length was 300 mm. Figure 1(a) shows the principle diagram of direct laser-filler wire welding of Al-Si coated PHS. The spot diameter was 0.92 mm, and there was no butt gap. Other welding parameters are shown in Table 4. After welding, the tailor-welded blanks #1~#5 and #7 were placed in a high-temperature furnace at 930°C for 300 seconds, while #6 at 950°C for 380 seconds, then stamped and quenched.

Metallographic and tensile samples were cut from the tailor-welded blanks, as shown in Figure 1(b). Metallographic samples were ground, polished, and then with 4% nitric acid alcohol for 5 seconds. The macroscopic appearance of the weld was observed using optical microscopy. The microstructure was examined using scanning electron microscopy. The chemical compositions were analyzed using an energy-dispersive X-ray energy spectrometer. Vickers microhardness was measured at 500 g load for 10 seconds. The tensile properties of the welded joints were tested using a universal tensile machine and

extensometer with a tensile speed of 3 mm/min. High-speed tensile testing was conducted using high-speed tensile test machines with loading rates of 100/s and 500/s.

Table 1. The chemical compositions of the as-received Al-Si coated PHSs (wt.%).

Serial number	Si	Mn	Cr	Al	Cu	Ni	Fe
#1	0.28	1.51	0.22	0.26	/	0.06	Bal.
#2	0.50	1.05	0.17	0.05	/	/	Bal.
#3	0.32	1.30	0.42	0.21	/	/	Bal.
#4	0.16	1.45	0.1	0.05	0.15	/	Bal.
#5	0.12	1.40	0.16	0.13	0.02	/	Bal.
#6	0.16	1.40	0.23	0.07	0.02	0.05	Bal.
#7	0.31	1.20	0.30	0.31	/	/	Bal.

Table 2. The thicknesses of the as-received Al-Si coated PHSs (mm).

Serial number	#1	#2	#3	#4	#5	#6	#7
Thickness	1.5	1.4	1.4	2.0	1.8	2.3	1.4

Table 3. The coating thicknesses of the as-received Al-Si coated PHSs (μm).

Serial number	#1	#2	#3	#4	#5	#6	#7
Upper coating thickness	31.36	24.02	11.63	31.22	39.08	31.7	32.12
Lower coating thickness	34.49	20.94	11.49	27.74	18.91	38.95	29.2

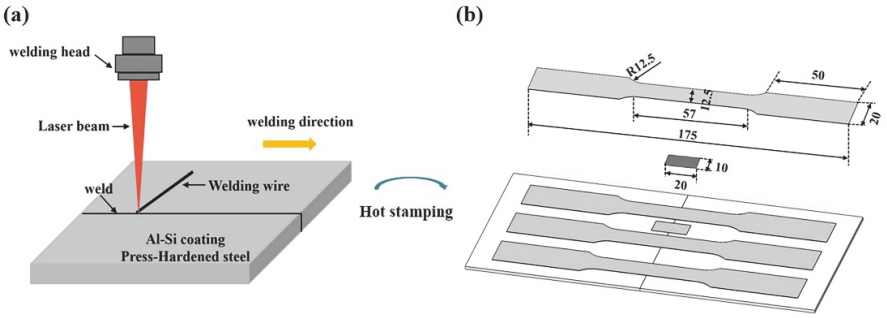

Fig. 1. (a) Schematic diagram of laser welding with filler wire (b) Schematic diagram of tensile sample (unit: mm).

Table 4. Welding parameters were used in this experiment.

	Laser power (W)	Welding speed (m/min)	Wire feeding speed (m/min)
#1	4800	5	3
#2	4800	5	3
#3	4800	5	3
#4	7200	5	5.5
#5	6800	5	5
#6	8200	5	6.4
#7	5200	5	3.4

3. Results and Discussion

3.1. *Weld section morphology*

The automotive industry strictly requires the ratio of the weld reinforcement to the plate thickness, usually within 15%-20%. The cross-sectional morphologies of seven WZs after welding are shown in Figure 2. The boundaries of the WZ could be observed. The upper and bottom reinforcements of the welds were measured using an optical microscope. According to Figure 3, the ratio of the upper or bottom reinforcements of each weld to the thickness of the plate was between 6% and 17%, with most falling between 6% and 15%. This suggested that the control of the weld reinforcement is appropriate.

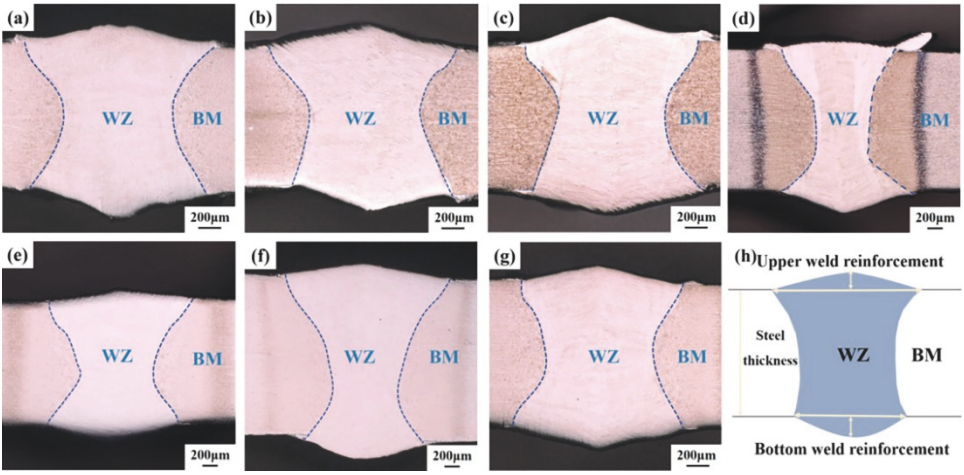

Fig. 2. (a) Optical image of weld #1 (b) Optical image of weld #2 (c) Optical image of weld #3 (d) Optical image of weld #4 (e) Optical image of weld #5 (f) Optical image of weld #6 (g) Optical image of weld #7 (h) Schematic diagram of weld reinforcement.

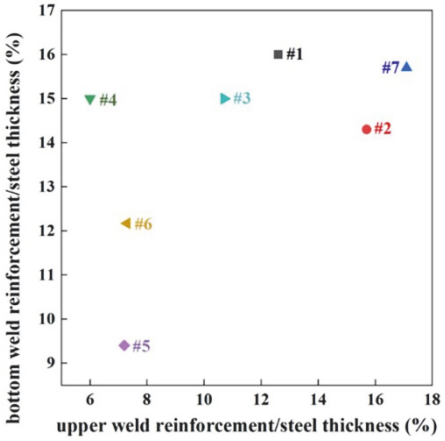

Fig. 3. Ratio of seven distinct weld reinforcements about their corresponding steel thicknesses.

The main component of Al-Si coating is aluminum, with a concentration typically exceeding 80%. Sun [20] *et al.* explored the evolution of Al-Si coating on the laser welding of Al-Si coated PHS and found that the Al-rich molten pool formed more δ-ferrite. Ferrite is responsible for the eventual failure of welded joints during early tensile testing. Figure 4 shows the weld zone morphology after hot stamping under direct laser-filler welding. There were no cracks and pores in the WZs. No apparent ferrite aggregation was observed in the WZs. This indicates that the direct laser-filler wire welding method effectively achieved a uniform distribution of alloying elements, especially Al, in the WZs.

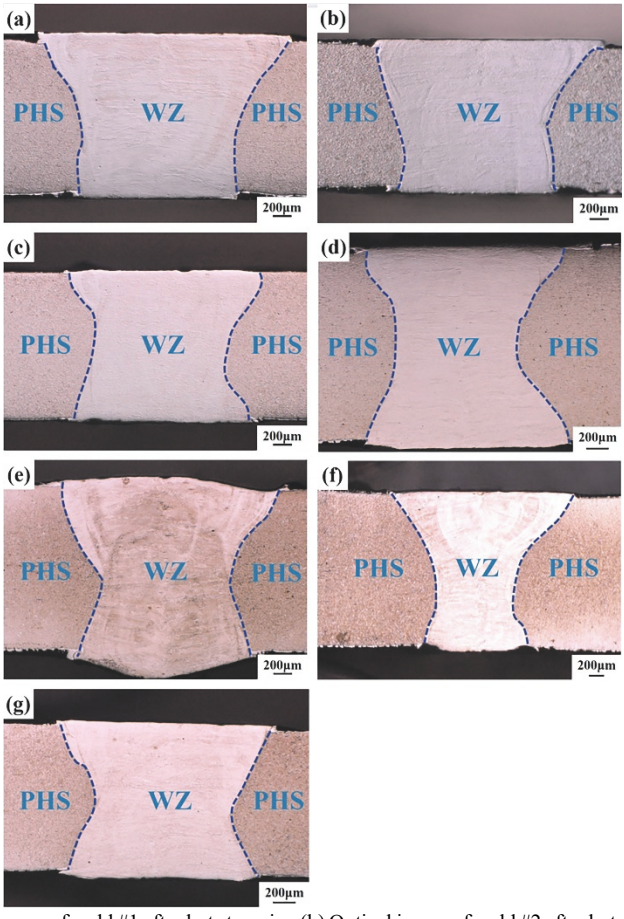

Fig. 4. (a) Optical image of weld #1 after hot stamping (b) Optical image of weld #2 after hot stamping (c) Optical image of weld #3 after hot stamping (d) Optical image of weld #4 after hot stamping (e) Optical image of weld #5 after hot stamping (f) Optical image of weld #6 after hot stamping (g) Optical image of weld #7 after hot stamping.

3.2. *Microstructure and chemical compositions of the welds*

The Al-Si coating was mixed with the molten pool during the laser welding process, and the distribution of Al affects the weld microstructure. When severe Al segregation occurred,

the weld fusion line region would exhibit a larger size of ferrite after hot stamping. The formation of ferrite deteriorates the mechanical properties of welded joints.

Xu [10] studied the direct laser-filler wire welding of 22MnB5 steel without removing the Al-Si coating and achieved full martensite at WZs. The Al content of martensite was 0.9-1.09 wt.%. Ferrite formation was significantly inhibited when the aluminum content in the weld was drastically reduced. Lin [19] *et al.* calculated the structural evolution of the weld with Al contents of 0.8 wt.%, 1.2 wt.%, and 1.6 wt.% using Jmatpro software. The results showed that the ferrite content decreased significantly with a decrease in Al content.

The microstructure of the weld fusion line in different weld joints and the Al content are shown in Figure 5. The Al content in the WZs was diluted by filler wire, and the average Al content in the WZs ranged from 0.6 wt.% to 1.3 wt.%.

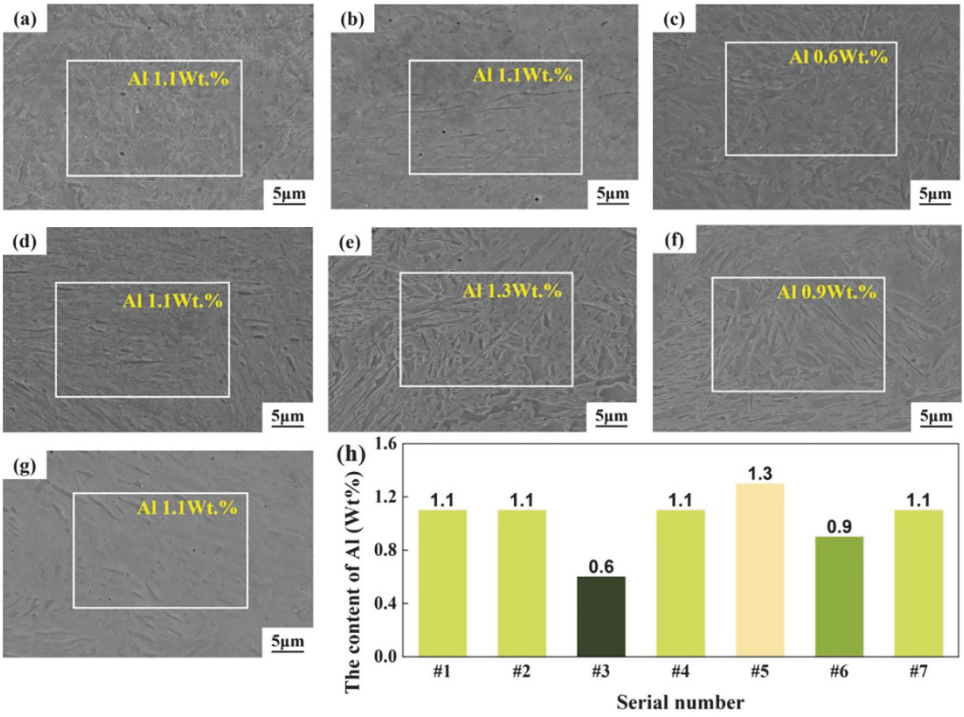

Fig. 5. (a) SEM image in weld fusion line of #1 weld (b) SEM image in weld fusion line of #2 weld (c) SEM image in weld fusion line of #3 weld (d) SEM image in weld fusion line of #4 weld (e) SEM image in weld fusion line of #5 weld (f) SEM image in weld fusion line of #6 weld (g) SEM image in weld fusion line of #7 weld (h) The content of Al in seven different weld joints.

3.3. *Mechanical Properties Tests*

Figure 6 (a) shows the typical appearance of the fractured specimens. All fracture areas are located in the base material region, suggesting that this method can achieve high-quality welds for welding various Al-Si coated PHSs. Tensile test results of the welded joints of different Al-Si coated PHSs are shown in Figure 6 (b). The tensile strength and elongation of 1500 MPa grade Al-Si coated PHSs exceeded 1500 MPa and 7%, respectively.

Martensite with a high dislocation density was the primary microstructure in the WZ with filler wire, significantly increasing PHS joints' tensile strength and elongation. Furthermore, high-quality welded joints have also been achieved for the higher strength 1700 MPa grade PHS with a tensile strength exceeding 1700 MPa and an elongation greater than 8%. Therefore, filling filler wire considerably enhanced the plasticity of the welded joints.

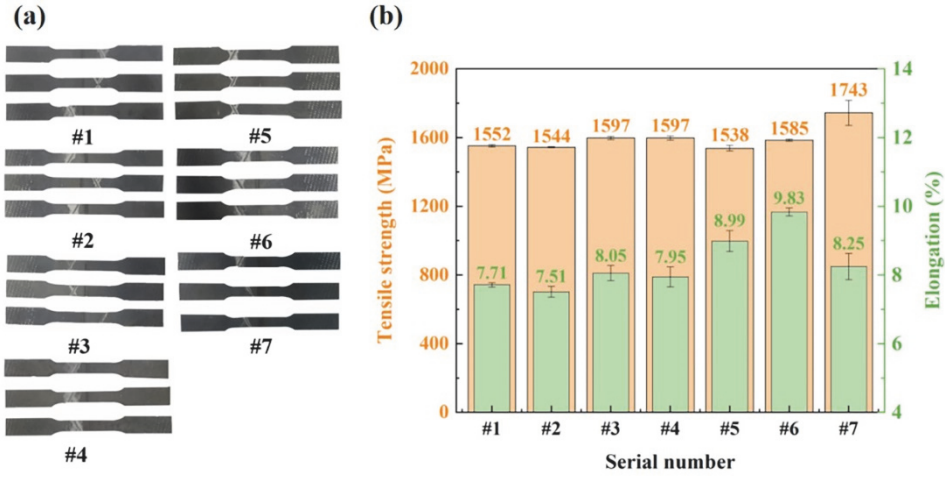

Fig. 6. (a) The appearances of the ruptured specimens (b) Tensile test results of seven different Al-Si coated PHSs laser welded joints.

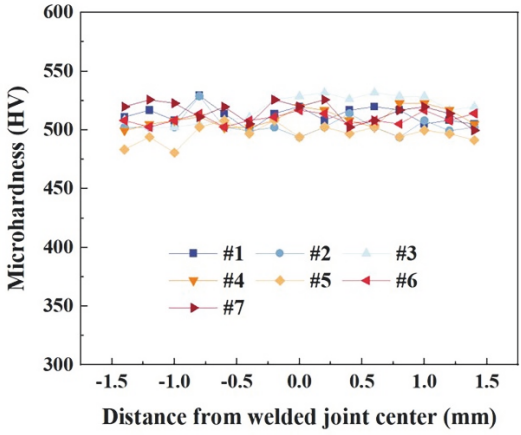

Fig. 7. Microhardness distribution of seven different Al-Si coated PHSs laser welded joints.

Figure 7 shows the microhardness distribution of the welded joints after hot stamping. The hardness was nearly the same as that of the HSBM due to the microstructure of the heat-affected zone being transformed into martensite. The filler wire diluted the Al content in the WZ and the austenite forming elements in the filler wire inhibited ferrite formation [21]. The microhardness of seven types of welded joints and their corresponding base materials were comparable, with values of approximately 500 HV.

In addition, high-rate tensile tests at 100/s and 500/s were conducted on #2 and #3 PHS welded joints. The two types of PHS, #2 and #3, have the same plate thickness and tensile strength, but #2 is typically thick-coated while #3 is thin-coated. The results indicated that the strength of the laser-welded joints could exceed 1,550 MPa at tensile rates of 100/s and 500/s (refer to Figure 8). Figure 9 shows the typical application of the welding technique in producing automotive components such as A-pillars, B-pillars, and one-piece door rings.

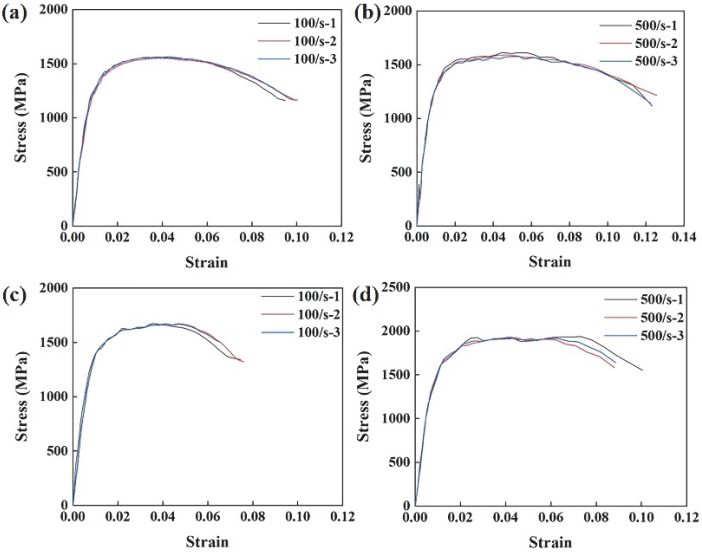

Fig. 8. (a) High Tensile test results for #2 at 100/s (b) High Tensile test results for #2 at 500/s (c) High Tensile test results for #3 at 100/s (d) High Tensile test results for #3 at 500/s.

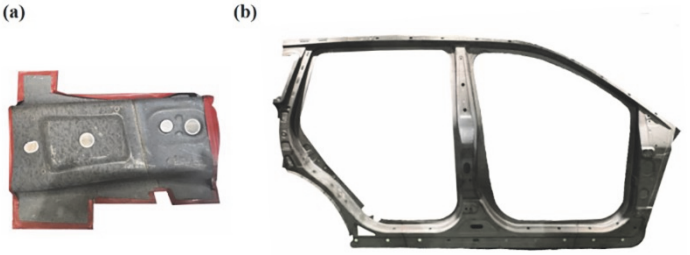

Fig. 9. (a) A part of laser-welded automotive B-pillar (b) The laser welded door ring by direct laser-filler wire welding after hot stamping.

4. Conclusion

In summary, our direct laser wire-filler welding can achieve high-quality weld joints for various PHSs without removing the Al-Si coating and setting the gap before laser welding. This process allows for the control of the microstructure in the WZ and reduces the formation of ferrite, ultimately enhancing the mechanical properties of the welded joints.

1) From the macrostructure of the weld metal, the weld reinforcement was controlled within 6% to 18%. After hot stamping, the tensile strength and elongation of the welded joint were over 1500 MPa and 7%, respectively. High-rate tensile tests on the welded joint of PHS with thick or thin Al-Si coating revealed that the tensile strength exceeded 1550 MPa and failed in BM.

2) No visible ferrite was observed in the WZ. The average content of Al in the WZ welded from seven various BMs was within 0.6%-1.3%. The average microhardness values in the WZs were comparable to that of the BM, which was around 500 HV.

3) Using the new wire dilutes the coating composition in the molten pool, reduces Al segregation in the fusion zone, decreases δ-ferrite generation, and enhances weld properties. This method is suitable for almost all types of laser tailor welding of Al-Si coated hot-formed steels with varying plate thicknesses, coating thicknesses, and base material strengths. It has also been utilized in the automotive industry for production purposes.

References

1. H. Karbasian and A. E. Tekkaya, A review on hot stamping, *Journal of Materials Processing Technology* **210**, 2103 (2010).
2. T. Taylor and A. Clough, Critical review of automotive hot-stamped sheet steel from an industrial perspective, *Mater Science and Technology* **34,** 809 (2018).
3. D. W. Fan and B. C. D. Cooman, State-of-the-knowledge on coating systems for hot stamped parts. *Steel Research International,* **83**, 412 (2012).
4. D. W. Fan, H. S. Kim, J. K. Oh, K. G. Chin and B. C. D. Cooman, Coating degradation in hot press forming, *ISIJ International*, **50**, 561 (2010).
5. Z. Wang, Z. H. Cao, J. F. Wang, and M. X. Huang, Improving the bending toughness of Al-Si coated press-hardened steel by tailoring coating thickness, *Scripta Materialia*, **192**, 19 (2021).
6. D. San Martin and Y. Palizdar, et al., Influence of Aluminum Alloying and Heating Rate on Austenite Formation in Low Carbon-Manganese Steels, *Metallurgical and Materials Transactions A*, **42**, 2591 (2011).
7. K. Ding, et al., Clarification of the ferrite formed in the laser welded joint of the Al–Si coated press-hardened steel, *Journal of Materials Research and Technology*, **23**, 5880 (2023).
8. D. C. Saha and E. Biro, et al., Fusion zone microstructure evolution of fiber laser welded press-hardened steels, *Scripta Materialia,* **121**, 18 (2016).
9. D. C. Saha and E. Biro, et al., Fiber laser welding of Al-Si-coated press-hardened steel, *Welding Journal*, **95**, 147 (2016).
10. W. Xu and Z. Jiang, et al., Direct laser-filler wire welding of Al–Si coated 22MnB5 steel without removing the Al–Si coating, *Journal of Materials Research and Technology*, **24**, 2265 (2023).
11. R. Vierstraete and W. Ethling, et al., Laser ablation for hardening laser welded steel blanks, *Industrial Laser Solutions*, **25**, 6 (2010).
12. W. Xu and S. Yang, et al., Effect of Al-Si Coating Removal State on Microstructure and Mechanical Properties of Laser Welded 22MnB5 Steel, *Journal of Materials Engineering and Performance*, **32**, 4205 (2023).

13. X. He and Y. Qin, et al., Effect of welding parameters on microstructure and mechanical properties of laser welded Al-Si coated 22MnB5 hot stamping steel, *Journal of Materials Processing Technology*, **270**, 285 (2019).
14. M. Kang and Y. Kim, et al., Effect of heating parameters on laser welded tailored blanks of hot press forming steel, *Journal of Materials Processing Technology*, **228**, 137 (2016).
15. J. Sun and Z. Han, et al., The segregation control of coating element for pulse fiber laser welding of Al-Si coated 22MnB5 steel, *Journal of Materials Processing Technology*, **286**,116833 (2020).
16. W. Xu and W. Tao, et al., Effect of oscillation frequency on the mechanical properties and failure behaviors of laser beam welded 22MnB5 weld, *Journal of Materials Research and Technology*, **22**,1436 (2023).
17. M. King and C. Kin, et al., Laser tailor-welded blanks for hot-press-forming steel with arc pretreatment, *International Journal of Automotive Technology*, **16**, 279 (2015).
18. X. Wang and Z. Zhang, et al., Effect of Ni foil thickness on the microstructure of fusion zone during PHS laser welding, *Optics & Laser Technology*, **125**, 106014 (2020).
19. W. Lin and F Li, et al., Effect of filler wire on laser welded blanks of Al-Si-coated 22MnB5 steel, *Journal of Materials Processing Technology*, **259**, 195 (2018).
20. Q. Sun, et al., Suppression of δ-ferrite formation on Al-Si coated press-hardened steel during laser welding, *Materials Letters*, **245**, 106 (2019).
21. M. S. Khan and A. Macwan, et al., α-ferrite Suppression during Laser Welding of Al-Si Coated 22MnB5 Press-Hardened Steel, *Welding Journal*, **100**, 213 (2021).

Open Access This chapter is licensed under the terms of the Creative Commons Attribution-NonCommercial 4.0 International License (http://creativecommons.org/licenses/by-nc/4.0/), which permits any noncommercial use, sharing, adaptation, distribution and reproduction in any medium or format, as long as you give appropriate credit to the original author(s) and the source, provide a link to the Creative Commons license and indicate if changes were made.

The images or other third party material in this chapter are included in the chapter's Creative Commons license, unless indicated otherwise in a credit line to the material. If material is not included in the chapter's Creative Commons license and your intended use is not permitted by statutory regulation or exceeds the permitted use, you will need to obtain permission directly from the copyright holder.